Hindawi
Mobile Information Systems
Volume 2021, Article ID 4482578, 9 pages
https://doi.org/10.1155/2021/4482578

Research Article

Musculoskeletal Rehabilitation Status Monitoring Based on sEMG

Xue Han,[1] Yan Zhao,[2] Feng Wang,[2] and Zun Liu[1]

[1]*Cangzhou Medical College, Cangzhou 061001, China*
[2]*Cangzhou Hospital of Integrated Traditional Chinese and Western Medicine (Hebei), Cangzhou 061012, China*

Correspondence should be addressed to Zun Liu; 20150199@stu.nmu.edu.cn

Received 22 September 2021; Accepted 18 October 2021; Published 2 November 2021

Academic Editor: Xingsi Xue

The reduction and improper movements in people's modern life will lead to physical discomfort, pain, and inflammation, which have generally affected the quality of people's daily life and work efficiency. The pain caused by improper movements are called musculoskeletal pain, which can be relieved or eliminated with treatment. Musculoskeletal disorders are actually one of the most common medical conditions, which affects approximately one quarter of all adults in the world. Although surface electromyography (sEMG) is an acknowledged technology in musculoskeletal rehabilitation study, it is considerably significant to monitor the musculoskeletal rehabilitation status based on sEMG. In order to monitor the musculoskeletal rehabilitation status, we combine fuzzy theory with neural network. This article proposes variable size, sliding window-based, generalized, dynamic, fuzzy neural network (GD-FNN), musculoskeletal rehabilitation status monitoring, that is, the window length of sliding window of sample data changes with the size of sample period. Finally, this study made a simulation on subjects, and the experimental results show that the proposed variable size, sliding window-based GD-FNN, musculoskeletal rehabilitation status monitoring method not only has good monitoring effect but also put on a good performance in root-mean-squared error (RMSE) and mean absolute percentage error (MAPE).

1. Introduction

Electromyography (EMG) signal is a kind of biological current signal, which is generated in any tissues and organs with muscle contraction [1, 2]. When the muscle is excited to contract, the muscle fiber also contracts. At the same time, there are some biochemical changes in the muscle fiber, as well as the change in the action potential. A waveform is formed if the change in the action potential is displayed by a real-time electromyographic electrode, which is called the electromyographic signal. From the perspective of signal analysis, it can also be called EMG. The EMG signal is derived from the person's own electrical signals with the characteristics of the direct and natural [3]. Currently, the EMG signal has become a kind of important information, which can be used for muscle movement [4], basic medical research, clinical diagnosis, muscle damage diagnosis [5], and rehabilitation medicine [6].

The EMG signal is a weak electrical signal, and skin and tissue have attenuation effect on EMG. The surface EMG (sEMG) signal collected on the skin surface is weaker than that collected by needle electrode [7, 8], and it is more susceptible to interference. The main problem to be considered is to eliminate the influence of noise and interference as far as possible and improve the fidelity of signal in the detection and recording of sEMG.

Musculoskeletal diseases or injuries, as well as the resulting long-term chronic pain and dysfunction [9], affect the quality of people's life around the world. With the improvement in people's awareness of exercise and protection, the severity of musculoskeletal injury and the risk of death are gradually reduced, but the incidence of acute or chronic musculoskeletal injury is still high. Musculoskeletal rehabilitation uses methods such as physical therapy to relieve pain, improve, or restore the musculoskeletal function, so as to improve the quality of life. Musculoskeletal injury covers various diseases affecting soft tissue, bone, and joints, which are common causes of long-term pain and physical disability [10]. So it

is important to monitor the musculoskeletal rehabilitation status based on sEMG signal.

Accordingly, the main contributions of this study are summarized as follows: (i) We study the acquisition of sEMG. (ii) We propose a variable size, sliding window-based, generalized dynamic fuzzy neural network (GD-FNN), musculoskeletal rehabilitation status monitoring.

The remaining of this article is organized as follows: Section 2 reviews the related work. In Section 3, we study the acquisition of sEMG. In Section 4, we propose a variable size, sliding window-based, GD-FNN, musculoskeletal rehabilitation status monitoring. The simulation results are shown in Section 5. Section 6 concludes this paper.

2. Related Work

Many strategies of sEMG have been proposed. Chen et al. [11] proposed an assembly torque monitoring method using sEMG and inertial signals. Fazeli et al. [12] had fabricated flexible dry electrodes to record the sEMG signals. Five hand motions were classified based on the sEMG signals recorded by their electrodes as well as commercially available wet rigid electrodes. Orban et al. [13] used a prosthetic hand precise control method to control the position of the prosthetic hand finger's motion depending on the sEMG signals as the control command; the controller used two different tuning methods genetic algorithm and Ziegler-Nichols. Tsinganos et al. [14] utilized the Hilbert space-filling curve for the generation of image representations of sEMG signals that were then classified by convolutional neural networks. Chen and Zhang [15] presented a method based on support vector machine to recognize hand gestures using sEMG. Karheily et al. [16] proposed a new approach for the identification of hand movements in order to control prosthetic hand. sEMG signals were used to identify movements using two frequency transforms: short time Fourier transform and Stockwell transform. Fatimah et al. [17] proposed an automatic recognition algorithm to identify hand movements using sEMG signals. The signals were decomposed into Fourier intrinsic band functions using the Fourier decomposition method. Li et al. [18] proposed an improved sEMG signal denoising method based on wavelet analysis, which combined the traditional wavelet threshold denoising method with the wavelet digital filter threshold denoising method made up the deficiency of the traditional wavelet denoising method. Kim et al. [19] developed a method to predict the grasping force from sEMG signals and various grasping postures. The proposed algorithm used a tensor algebra to train a multifactor model relevant to sEMG signals corresponding to various grasping forces and postures of the wrist and forearm in multiple dimensions. Liang et al. [20] proposed a novel study for gesture identification using sEMG signal, and the raw sEMG signal and the sEMG envelope signal were collected by the sensor at the same time. An efficient method of gesture identification based on the combination of two signals using supervised learning and univariate feature selection was implemented. Lin et al. [21] proposed two data-augmentation approaches to expend their sEMG data set, which were the simulation of the surface electrodes displacement on the skin and the muscle fatigue.

There have been many musculoskeletal rehabilitation methods studied for EMG signal. Kawase t al. [22] developed a hybrid system with electroencephalogram and EMG signals, and the EMG signals were used to estimate the joint angles. Peña et al. [23] proposed a multilayer perceptron neural network to map the EMG signals to the user's torque, and an EMG-driven adaptive impedance control was proposed to improve the user participation during the rehabilitation session. Pan et al. [24] designed an EMG-driven neural-machine interface based on a musculoskeletal model. Kapelner et al [25] proposed a myoelectric control method based on neural data regression and musculoskeletal modeling, which used the timings of motor neuron discharges decoded by high-density sEMG decomposition to estimate muscle excitations.

The generalized dynamic fuzzy neural network (GD-FNN) has also been studied. Yen [26] proposed to use the characteristics among moments and fuzzy rules to identify the density function in advance. Wu et al. [27] presented a fast approach for automatically generating fuzzy rules from sample patterns using GD-FNN.

3. Acquisition of sEMG

In order to monitor the musculoskeletal rehabilitation status, it is necessary to acquire the sEMG. By fixing the surface electrodes on the arms, body, and legs, the sEMG signal acquisition system is composed of surface electrode, data acquisition amplifier circuit, and digital signal processing (DSP) to acquire sEMG signal. The sEMG signal has the following characteristics. (i) The sEMG signal is a type of alternating current (AC) voltage that is roughly proportional in magnitude to the strength generated by the muscles. (ii) The sEMG signal is a weak electrical signal, whose amplitude range is generally between 0 and 5 mV, that is, 20–300 μV. (iii) When surface electrodes are used, the energy of sEMG signal is mainly concentrated below 1000 Hz, and the spectrum is distributed between 20 Hz and 500 Hz. The spectrum is concentrated between 50 Hz and 150 Hz. The maximum frequency of the power spectrum depends on the muscle, which is usually between 30 Hz and 300 Hz. (iv) Frequency-domain parameters can better reflect sEMG characteristic than time-domain parameters. Because when the magnitude of the strength changes slightly, the time-domain waveform changes greatly, whereas the frequency-domain characteristic changes relatively small. (v) The shape of amplitude spectrum frequency characteristic curve is similar when the same muscle is doing different movements. Therefore, according to the characteristics of sEMG signal, its collection system should be able to acquire weak sEMG signal and amplify it, which can also shield interference and filter clutter so as to get useful sEMG signal.

3.1. The Placement of Surface Electrode. The electrode used in this study is three-point differential input electrode, and the acquisition electrode and grounding electrode are silver chloride-silver electrodes. Basically, a grounding electrode is a conductive object that establishes a direct connection to

the ground. Before placing the electrode, the following preparations should be made. At first, in order to ensure a good contact between the electrode and the skin, we should wipe the electrode with medical alcohol to remove the dead skin and oil on the skin surface and minimize the impedance between the electrodes [28]. Then placing the electrode in the direction of the muscle fiber. It should be avoided to be placed on or adjacent to the tendon because the muscle fibers become thinner when they are close to the tendon, and the number of muscle fibers is also reduced, which leads to the reduction in the amplitude of the sEMG signal. Finally, the electrode is fixed with a fixed belt to reduce the power frequency.

3.2. Data Acquisition Amplifier Circuit. Because the sEMG signal may be weak, the sEMG signal of human body is only mV level. It is easy to be affected by external electric field and circuit noise in transmission. Therefore, the design of the acquisition circuit should not only consider the amplification of the signal but also fully consider how to remove the interference and acquire useful sEMG signal. The following problems should be considered in designing sEMG amplifier circuit: (i) The gain of the amplifier should be high. The amplitude of sEMG signal is between 0 and 5 mV, which is an extremely weak electrical signal. It needs to be amplified to about 1 V for use. Therefore, the amplification factor of the amplifier should be set between 100 and 1000. (ii) The common-mode rejection ratio (CMRR) of the circuit should be high. The acquisition of sEMG is susceptible to interference from 50 Hz power supply and other high-frequency electrical noise. However, these interference signals are represented as the same amplitude and phase signal-common-mode signal at the input end of the amplifier, so the high CMRR amplifier circuit can be used to suppress the common-mode interference signal. (iii) The input impedance of the electrode is higher than the contact impedance between electrode and skin. The range of possible contact impedance between skin and electrode could be very wide up to 2MΩ in dry areas. Therefore, under similar conditions, even if the CMRR of the amplifier is very good, if the input impedance is not high enough, the common-mode interference signal will still cause a large output error, so it is necessary to improve the input impedance of the amplifier. The amplifier circuit used in this study is a hierarchical amplifier circuit, and the basic circuit diagram is shown in Figure 1.

The sEMG signal is amplified step by step and input into the filter in the amplification process. After filtering useless signals, interference, and noise frequency through low-pass and high-pass filters, the 50 Hz power frequency signal is filtered through the notch filter. By the amplification and acquisition of sEMG signal, we can get better sEMG signal for the following acquisition.

3.3. The Analysis and Solution of Interference Sources and Noise. Due to the sEMG signal is very weak, in the process of signal acquisition, it is inevitable to introduce multiple interferences in signal acquisition, so that the useful sEMG signal is submerged in interference noise. Thus, it is important to distinguish and eliminate interference correctly in sEMG signal acquisition. It can be said that the effective interference suppression is the most critical part of the whole system. In this study, interference sources and characteristics are analyzed, and the solution is provided to reduce interference.

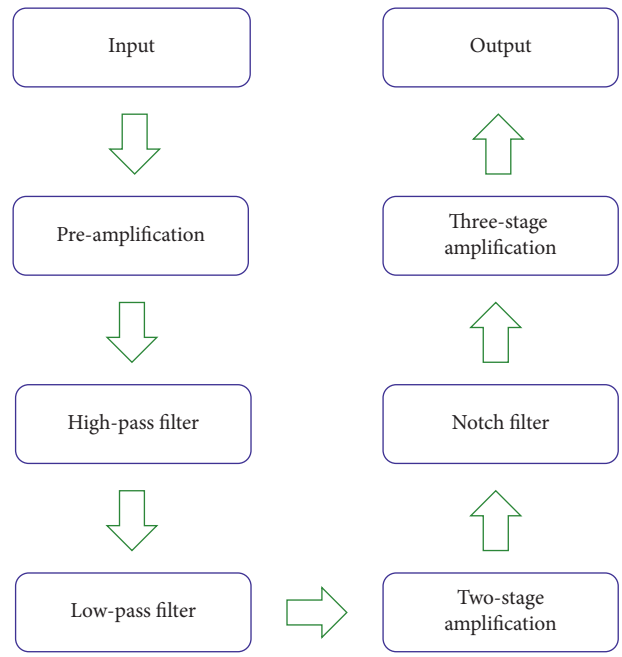

Figure 1: The diagram of amplifier circuit.

3.3.1. 50 Hz Power Frequency Interference. The interference of 50 Hz power frequency comes from the main power supply. The interference is obvious when closing to the power supply. Usually, 50 Hz power frequency interference is the most frequent and largest interference in the experiment. The easiest way to reduce interference of 50 Hz is to use shielded cable for electrode connection, which can also shorten the length of cable as much as possible to reduce interference.

3.3.2. High-Frequency Interference. High-frequency interference comes from radio stations, wireless communication facilities, and other instruments. The frequency of these signals is far beyond the sEMG signal band, which usually does not directly cause interference. However, when there is bad electrode contact or high-frequency signal, low-frequency signal can be generated due to "detection" and high-frequency "clipping interference." The solution is to add low-pass filter to filter out high-frequency interference signal.

3.3.3. Other Bioelectrical Signals. Signal and interference are opposite, and sEMG signal is regarded as interference when electrocardiogram (ECG) is acquired. ECG is also considered interference when sEMG signal is acquired. Therefore,

other bioelectrical signals can be regarded as interference, which should also be eliminated.

3.3.4. Background Noise. Background noise mainly comes from the voltage and current generated by the electronic components of the amplifier, which is generally related to the quality and performance of the components inside the amplifier. In the input circuit, noise will also be introduced, and its size is related to electrode potential and contact resistance [29]. Consequently, in the selection of amplifier, we should choose high-quality electronic components to reduce noise.

3.3.5. The Stimulus Artifact. The stimulus artifact is present whether or not the nerve is in the tube, although its form may be altered by the electrical properties of the nerve. The essence of stimulus artifact is the electric stimulus signal directly recorded by the amplifier. It is transmitted to the recording end in an electric way, which is a purely physical process. Too much stimulus artifact will interfere with subsequent sEMG signal. The stimulus artifact can be reduced by isolating the output and narrowing the distance between the stimulus electrodes.

3.4. Feature Extraction and Data Normalization. The time-domain characteristics of sEMG are often used to analyze the correlation between sEMG and muscle activity in the study of human motor function based on sEMG. The time-domain characteristics of sEMG signal change obviously during muscle contraction. It is generally considered that the temporal characteristics of sEMG signal have a significant correlation with muscle contraction force. This study uses sEMG time-domain characteristics to describe muscle activity. The common characteristics of sEMG time-domain analysis are shown as follows.

Root mean square (RMS) can better reflect the discharge quantity of motor neurons in unit time, which is defined as follows:

$$\mathrm{RMS} = \sqrt{\frac{\int_t^{t+T} \mathrm{sEMG}^2(\mathrm{t})\mathrm{d}t}{T}}, \tag{1}$$

where sEMG (t) is the time-domain amplitude change curve of sEMG signal. T and t are the selected test period and start time, respectively.

sEMG signal is derived from the electrical stimulation pulse generated by motor neuron. Zero crossing (ZC) is related to the frequency of the pulse that can be used to represent the strength of muscle contraction, which is defined as follows:

$$\mathrm{ZC} = \sum_{k=1}^{K} \mathrm{sgn}\left(-x_k \cdot x_{k+1}\right), \tag{2}$$

where sgn (x) is the sign function, when $x > 0$, sgn (x) = 1, and when $x \le 0$, sgn (x) = 0.

Integrated sEMG (i_sEMG) can reflect the strength of muscle activity during the integral period. Meanwhile, the i_sEMG will change with the muscle strength, which is calculated as follows:

$$i\_\mathrm{sEMG} = \int_t^{t+T} \mathrm{sEMG}(t)\mathrm{d}t. \tag{3}$$

Wavelength (WL) is the calculation of waveform length in an analysis window, which can reflect the duration of sEMG.

$$\mathrm{WL} = \frac{1}{P}\sum_{m=1}^{P} |x(m+1) - x(m)|, \tag{4}$$

where P is the period of signals.

4. Musculoskeletal Rehabilitation Status Monitoring Based on GD-FNN

In order to monitor the musculoskeletal rehabilitation status, this study combines fuzzy theory with neural network, that is, GD-FNN, which makes the new network structure monitoring more ideal. Besides, GD-FNN can be used for linear modeling, which has good nonlinear mapping ability. The GD-FNN can adjust parameters and identify structures at the same time. In this network algorithm, fuzzy rules are selected dynamically and used to determine the width of Gaussian function to avoid randomness of initial parameter selection. Compared with other networks, it is easier to implement, even though the GD-FNN is more complex.

4.1. GD-FNN-Based Musculoskeletal Rehabilitation Status Monitoring. This study uses GD-FNN to monitor the musculoskeletal rehabilitation status based on sEMG. The whole musculoskeletal rehabilitation status monitoring network is divided into four layers. The first layer is input layer, whereas the second layer is fuzzy layer, which converts the data input in the first layer into the corresponding fuzzy statement. The membership of each input variable to the fuzzy statement generated by the network is calculated by the membership function, which provides a basis for the selection of fuzzy rules in the next layer. The membership function is expressed by Gaussian function.

Assuming that input variable x_m ($m = 1, 2, \ldots, q$), q is the number of input variables, and each input x_m has s membership function A_{mn} ($n = 1, 2, \ldots, s$), and we have

$$g_{mn}(x_m, c, \sigma) = \exp\frac{-(x_m - c_{mn})^2}{2\sigma_{mn}^{\ 2}}, \quad m = 1, 2, \ldots, q, n = 1, 2, \ldots, s, \tag{5}$$

where $g_{mn}(x_m, c, \sigma)$ is the nth membership degree function of x_m. c_{mn} and σ_{mn} are the center and width of the membership function, respectively.

The third layer is the rule layer, which mainly adjusts the existing rules and modifies the center and width of the membership function through network training. The third layer calculates the nth fuzzy rule weight of the mth variable R_{mn} ($n = 1, 2, \ldots, s$).

$$\varphi_{mn}(x_1, x_2, \ldots, x_s) = \exp\left[-\sum_{n=1}^{q} \frac{(x_m - c_{mn})^2}{2\sigma_{mn}^2}\right], \quad n = 1, 2, \ldots, s. \tag{6}$$

The fourth layer is the output layer. The rule output weights of the previous layer are weighted and summed, and the fuzzy language is defuzzified to get the system network output variables.

$$y(x_1, x_2, \ldots, x_q) = \sum_{n=1}^{s} \omega_n \cdot \varphi_n, \tag{7}$$

where y is the value of an output variable, and ω_n is the connection weight corresponding to the nth rule.

4.2. Variable Size Sliding Window-Based GD-FNN Musculoskeletal Rehabilitation Status Monitoring. The learning algorithm of GD-FNN is based on hierarchical, online, self-organizing learning strategy, which aims at reducing the adjustment in the following learning period. Therefore, the training samples of GD-FNN are randomly sampled, and the sample data of musculoskeletal rehabilitation status monitoring is continuous data. The original learning algorithm abstracts the training samples globally and only pays attention to the randomness of the samples while ignoring the periodicity of the samples. Therefore, this study proposed variable size, sliding window-based, GD-FNN, musculoskeletal rehabilitation status monitoring, that is, the window length of sliding window of sample data changes with the size of sample period, which enables the monitoring network to have "periodicity" in samples.

Let the period of the training sample be T_m (m is the number of periods), and the length L_{sw} of the sliding window changes with the length of each sample period, that is, $L_{sw} = [T_1, T_2, \ldots, T_m]$. When receiving new data, if the number of samples reaches the length of the first sliding window, then the method returns to the previous step and takes the network parameters generated by the current window as the initial parameters of the training network in the next window. Otherwise, when the first sample data enters the monitoring model, the fuzzy neural network generates the first rule and determines the parameters of the rule. The matching degree and output error of ($X_1, \ldots, X_r$; $t_1, \ldots, t_r$) fuzzy rules of observation data is calculated to determine whether to generate new fuzzy rules. X is the sample input, which includes the RMS of sEMG, i_sEMG, and joint angle, and t is the expected output of musculoskeletal rehabilitation status monitoring.

4.2.1. The Generation Criteria of Fuzzy Rule. The completeness of GD-FNN musculoskeletal rehabilitation status monitoring fuzzy rules indicates that the fuzzy system is considered with completeness if the matching degree between the input and at least one fuzzy rule is not less than λ within a certain variation interval. That is, if the subsequent samples meet the completeness of fuzzy rules, GD-FNN musculoskeletal rehabilitation status monitoring does not need to add new rules, which only needs to adjust the parameters of existing fuzzy network rules. The method uses the calculation of Mahalanobis distance to distinguish the matching degree of fuzzy rules, which represents the Mahalanobis distance $\mathrm{md}_r(n)$ between sample data X_r and the current radial basis function unit center.

$$\mathrm{md}_{r(\min)} = \mathrm{md}_r(N) > r_d, \tag{8}$$

$$N = \arg\min_{1 \le n \le s} (\mathrm{lgmd}_r(n)), \tag{9}$$

$$\mathrm{md}(n) = \sqrt{(X - C_n)^T \eta \sum_{n}^{-1} (X - C_n)}, \tag{10}$$

where equation (10) is Mahalanobis distance, and $\mathbf{X} = (x_1, \ldots, x_q)^T \in Q^q$, $\mathbf{C}_n = (c_{1n}, c_{2n}, \ldots, c_{qn}) \in Q^q$. At the same time, $\sum$-1 n is defined as follows:

$$\sum_{n}^{-1} \begin{bmatrix} \frac{1}{2\sigma_{1n}^2} & 0 & \cdots & 0 \\ 0 & \frac{1}{2\sigma_{2n}^2} & 0 & 0 \\ 0 & 0 & \ddots & 0 \\ 0 & \cdots & 0 & \frac{1}{2\sigma_{qn}^2} \end{bmatrix}, \quad n = 1, 2, \ldots, s. \tag{11}$$

If equation (8) is valid, it is considered that the rules of the current system do not meet the completeness, and it is necessary to consider adding a new rule. Meanwhile, r_d will change with the sample input number k in the monitoring process, and the adjustment range is defined as follows:

$$r_d = \begin{cases} d_{\max} = \sqrt{\ln\left(\frac{1}{\lambda_{\min}}\right)}, & 1 < r < \frac{k}{4}, \\ \max[d_{\max} \times \lg\delta^r, d_{\min}], & \frac{k}{4} \le r \le \frac{3k}{4}, \\ d_{\min} = \sqrt{\ln\left(\frac{1}{\lambda_{\max}}\right)}, & \frac{3k}{4} < r \le k, \end{cases} \tag{12}$$

where r is the number of monitoring, and $\delta = (d_{\min}/d_{\max})^{4/k}$ is the attenuation constant.

Similar to the completeness of fuzzy rules, the output error of GD-FNN musculoskeletal rehabilitation status monitoring is also used as the basis to judge whether new fuzzy rules need to be added. According to equations (6) and (7), the output of the network under the current structure is y_r, and the system error is defined as follows:

$$\|e_r\| = \|t_r - y_r\|. \tag{13}$$

If the error $||e_r||$ is greater than r_e, a new fuzzy rule needs to be considered in the monitoring. Here, r_e is a predefined

threshold that changes gradually during the monitoring process according to the following criteria:

$$r_e = \begin{cases} e_{\max}, & 1 < r < \dfrac{k}{4}, \\ \max\left[e_{\max} \times \lg\gamma^{k}, e_{\min}\right], & \dfrac{k}{4} \le r \le \dfrac{3k}{4}, \\ e_{\min}, & \dfrac{3k}{4} < r \le k, \end{cases} \tag{14}$$

where $e_{\min}$ is the minimum error desired by the output of GD-FNN musculoskeletal rehabilitation status monitoring, and $e_{\max}$ is the maximum error allowed by the system. r is the number of monitoring, and $\gamma = (e_{\min}/e_{\max})^{4/k}$ is the convergence constant that ranges from 0 to 1. In the study by Ma et al. [30], the convergent operation used a clustering strategy, which motivated this study in convergence.

4.2.2. Parameters Correction of Gaussian Membership Function. According to the generation criteria of fuzzy rules, when $||e_r|| > r_e$ and $\mathrm{md}_{r\,(\min)} > r_d$, a new fuzzy rule will be added to the system. However, when $||e_r|| > r_e$ and $\mathrm{md}_{r\,(\min)} > r_d$, although the current fuzzy rules can describe the observation data, the existing radial basis function unit does not contain the observation data X_r, which will degrade the monitoring performance of the network. Therefore, there is a rule that minimizes the Mahalanobis distance between the samples for a new sample X_r. If the conditions $||e_r|| > r_e$ and $\mathrm{md}_{r\,(\min)} > r_d$ are both valid, and the sample X_r is decomposed into the corresponding one-dimensional input variable x_m ($m = 1, 2, \ldots, q$), then the width of membership function of its nearest fuzzy rule ψ_{mn} ($n = 1, 2, \ldots, s$) can be adjusted as follows.

$$\psi'_{mn} = \xi \times \psi_m, \tag{15}$$

where ψ'_{mn} is the updated width, and $\xi \in (0, 1)$ is the attenuation factor.

5. Simulation and Results Analysis

The input parameters of variable size, sliding window-based, GD-FNN, musculoskeletal rehabilitation status monitoring are RMS, i_sEMG, and joint angle of sEMG, which are used to reflect the muscle activation degree.

5.1. Parameters Setting. The expected output accuracy of variable size, sliding window-based, GD-FNN, musculoskeletal rehabilitation status monitoring $e_{\min} = 0.06$ and maximum error $e_{\max} = 1$. The matching degree of fuzzy rule completeness $\lambda_{\min} = 0.6$ and $\lambda_{\max} = 0.9$. The threshold of error reduction rate $r_{\mathrm{err}} = 0.003$. Gaussian width attenuation factor $\xi_{\min} = q_d = 0.9$. Meanwhile, root-mean-squared error (RMSE) and mean absolute percentage error (MAPE) are used as performance indicators to judge the monitoring effect, which are defined as follows:

$$\mathrm{RMSE} = \sqrt{\frac{1}{K}\sum_{m=1}^{K}(e(m) - a(m))^2}, \qquad \mathrm{MAPE} = \frac{1}{K}\sum_{m=1}^{K}\left|\frac{e(m) - a(m)}{e(m)}\right|, \tag{16}$$

where K is the number of samples, and $e(m)$ and $r(m)$ are the mth expected output and actual output, respectively.

We choose improved particle swarm optimization combined with fuzzy neural network (IPSO-FNN) [31], expert opinion and fuzzy neural network (EO-FNN) [32], and interval type-2 fuzzy neural network (IT2FNN) [33] for comparison. RMSE is sensitive to large errors in data. The mean absolute error is the average of the absolute value of the deviation from the arithmetic mean of all individual observations. No positive and negative cancellations will occur because the error is absolutely validated. Therefore, RMSE and MAPE can well reflect the accuracy of the monitoring.

5.2. Comparison Analysis. sEMG of subjects is acquired to monitor musculoskeletal rehabilitation status. The sample space contains data from the subjects' five exercise periods. Figure 2 shows the monitoring effect of samples. The ordinate is the normalized muscle strength, and the abscissa is the number of samples. We take muscle strength as the research object of musculoskeletal rehabilitation status monitoring. The curves in Figure 2 are the desired and actual monitoring values of musculoskeletal rehabilitation status monitoring, respectively. From Figure 2, the muscle is stretched in the initial state, and the muscle fiber length is greater than the optimal muscle fiber length. The muscle length gradually decreases with the increasing joint angle; at the same time, the muscle strength increases gradually. When the muscle fiber length reaches the optimal length, the muscle strength reaches the maximum value. Muscle fiber begins to contract with continued movement; at this time, the muscle strength declines gradually. When the joint flexes to the maximum angle, the muscle strength increases with the increasing of muscle fiber length. When the joint reaches the optimal length, the muscle strength reaches the peak again and continues to stretch, and the muscle strength begins to decline until the movement reaches the initial angle.

In order to verify the effectiveness of the proposed method, the muscle strength monitoring effect of the proposed method is compared with other three baselines using the sample data of one of the subjects.

As can be seen from Figure 3, the monitoring error of muscle strength of IPSO-FNN is greater than other three baselines. Although the monitoring error of muscle strength of proposed method is the smallest, the curve of proposed method almost coincided with that of the desired output. The monitoring error of muscle strength of IPSO-FNN and EO-FNN are not so good as the proposed method in performance. Furthermore, in order to verify the stability of the

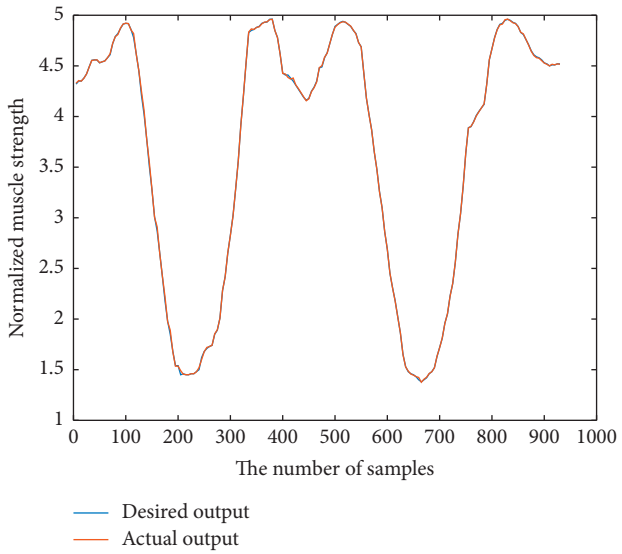

Figure 2: The monitoring effect of samples.

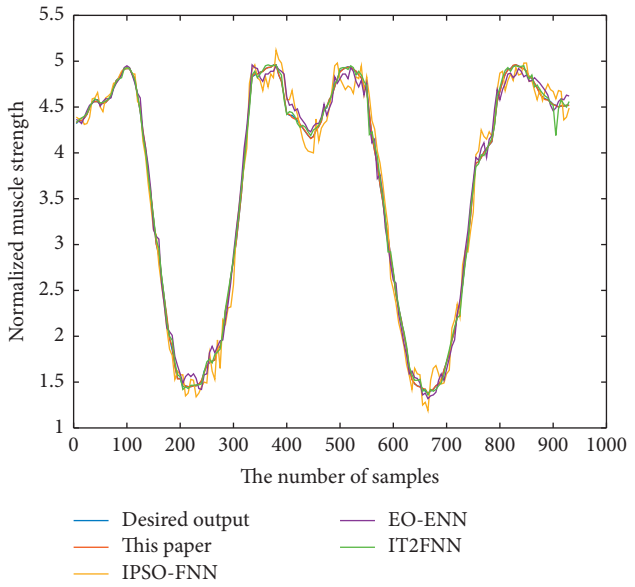

Figure 3: The comparison of monitoring method in normalized muscle strength.

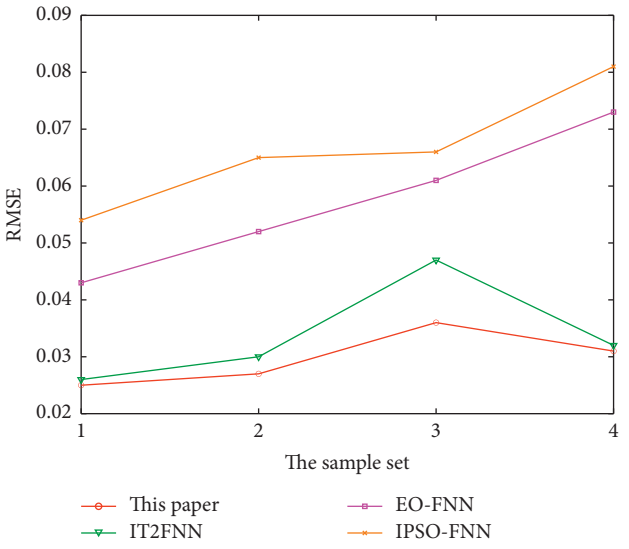

Figure 4: The comparison of RMSE.

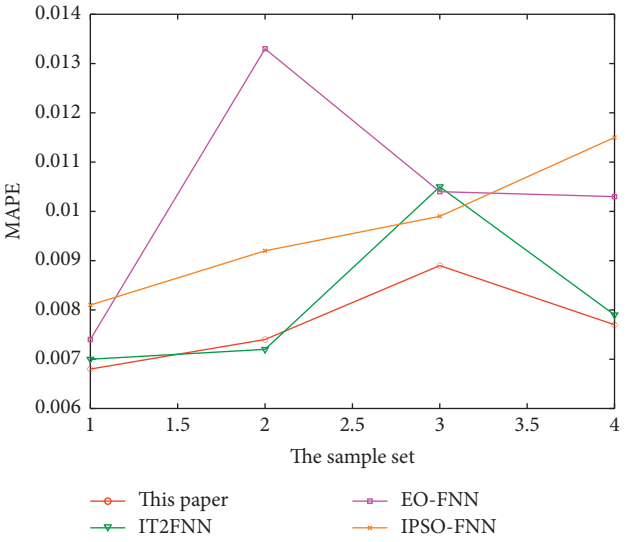

Figure 5: The comparison of MAPE.

proposed method, the MAPE and RMSE of the monitoring results of the three methods are compared with the data of the same subject's four movements as an example. Figures 4 and 5 show the comparison results.

According to Figures 4 and 5, the MAPE of the variable size, sliding window-based, GD-FNN, musculoskeletal rehabilitation status monitoring method is smaller than other three baselines. Meanwhile, it can be seen from the RMSE curve that the monitoring error of the proposed method always changes within a small range. Compared with the other three baselines, the variable size, sliding window-based, GD-FNN, musculoskeletal rehabilitation status monitoring method can make the monitoring results more stable.

6. Conclusions

Musculoskeletal pain is pain that affects the muscles and bones. People with musculoskeletal pain sometimes complain that their whole bodies ache. Different types of treatment and movement can be used to treat people with ache. However, the musculoskeletal rehabilitation status can be monitored based on sEMG. In this study, a variable size, sliding window-based GD-FNN is proposed to monitor musculoskeletal rehabilitation status, that is, the window length of sliding window of sample data changes with the size of sample period. The experimental results demonstrate that the proposed method has a good performance in normalized muscle strength monitoring.

The study on musculoskeletal rehabilitation status monitoring is a preliminary attempt. The subjects selected

are all relatively young men and convalescent patients who can exercise autonomously, and their body shape is relatively similar. Whether the musculoskeletal rehabilitation status monitoring method can be applied to all people and even patients with dyspraxia still needs further research. In addition, this study does not take into account the strength explosion of synergistic sEMG. In the future, it is necessary to consider the sEMG of synergistic muscle near the muscle on the basis of strength explosion monitoring of musculoskeletal rehabilitation status.

Data Availability

All data used to support the findings of the study is included within the article.

Conflicts of Interest

The authors declare that they have no conflicts of interest.

Authors' Contributions

Xue Han and Yan Zhao contributed equally to this work.

Acknowledgments

This study was supported by Cangzhou Key Research and Development program Guidance Project (Grant nos. 172302187 and 172302178).

References

[1] O. L. Zernov and E. A. Zhilenkova, "Classification algorithm of electromyography signals," in *Proceedings of The 2019 Ieee Conference of Russian Young Researchers In Electrical and Electronic Engineering (EICONRUS)*, pp. 1250–1253, Saint Petersburg, Russia, January 2019.

[2] M. Piasecki, O. Garnés-Camarena, and D. W. Stashuk, "Near-fiber electromyography," *Clinical Neurophysiology*, vol. 132, no. 5, pp. 1089–1104, 2021.

[3] M. Z. Jamal, D. H. Lee, and D. J. Hyun, "Real time adaptive filter based EMG signal processing and instrumentation scheme for robust signal acquisition using dry EMG electrodes," in *Proceedings of the 2019 16th International Conference On Ubiquitous Robots (UR)*, pp. 683–688, Jeju, South Korea, June 2019.

[4] S. A. Raurale, J. McAllister, and J. M. del Rincon, "Real-time embedded EMG signal analysis for wrist-hand pose identification," *IEEE Transactions on Signal Processing*, vol. 68, pp. 2713–2723, 2020.

[5] A. Hossen, G. Deuschl, S. Groppa, U. Heute, and M. Muthuraman, "Discrimination of physiological tremor from pathological tremor using accelerometer and surface EMG signals," *Technology and Health Care*, vol. 28, no. 5, pp. 461–476, 2020.

[6] C. Zhang, J. Zou, and Z. Ma, "Identification and analysis of limb rehabilitation signal based on wavelet transform," *Traitement du Signal*, vol. 38, no. 3, pp. 689–697, 2021.

[7] Y. Narayan, "SEMG signal classification using KNN classifier with FD and TFD features," *Materials Today: Proceedings*, vol. 37, pp. 3219–3225, 2021.

[8] G. Chen, W. Wang, Z. Wang, H. Liu, Z. Zang, and W. Li, "Two-dimensional discrete feature based spatial attention CapsNet for sEMG signal recognition," *Applied Intelligence*, vol. 50, no. 10, pp. 3503–3520, 2020.

[9] M. G. L. Monaco, L. Fiori, A. Marchesi et al., "Biomechanical overload evaluation in manufacturing: a novel approach with sEMG and inertial motion capture integration," in *Proceedings of the 20th Congress of the International Ergonomics Association (IEA 2018): Volume I: Healthcare Ergonomics*, vol. 818, pp. 719–726, Florence, Italy, August 2018.

[10] S. Yu, H. Jiang, and C. Lin, "The prediction of ankle injury based on sEMG using cerebellar model neural network," in *Proceedings of the 2019 International Conference On Fuzzy Theory And Its Applications (Ifuzzy)*, pp. 193–198, New Taipei, Taiwan, November 2019.

[11] C. Chen, K. Huang, D. Li, Y. Pan, Z. Zhao, and J. Hong, "Assembly torque data regression using sEMG and inertial signals," *Journal of Manufacturing Systems*, vol. 60, pp. 1–10, 2021.

[12] M. Fazeli, F. Karimi, V. Ramezanian, A. Jahanshahi, and S. Seyedin, "Hand motion classification using semg signals recorded from dry and wet electrodes with machine learning," in *Proceedings of the 28th Iranian Conference On Electrical Engineering (ICEE)*, pp. 710–713, Tabriz, Iran, August 2020.

[13] M. Orban, X. Zhang, Z. Lu, A. Marcal, A. Emad, and G. Masengo, "Precise control method on prosthetic hand using sEMG signals," in *Proceedings of the 2020 10th Institute Of Electrical And Electronics Engineers International Conference On Cyber Technology In Automation, Control, And Intelligent Systems (IEEE-CYBER 2020)*, pp. 326–331, Xi'an, China, October 2020.

[14] P. Tsinganos, B. Cornelis, J. Cornelis, B. Jansen, and A. Skodras, "A Hilbert curve based representation of sEMG signals for gesture recognition," in *Proceedings of the 2019 International Conference On Systems, Signals And Image Processing (IWSSIP 2019)*, pp. 201–206, Osijek, Croatia, June 2019.

[15] W. Chen and Z. Zhang, "Hand gesture recognition using sEMG signals based on support vector machine," in *Proceedings of the 2019 IEEE 8th Joint International Information Technology And Artificial Intelligence Conference (ITAIC 2019)*, pp. 230–234, Chongqing, China, May 2019.

[16] S. Karheily, A. Moukadem, J. B. Courbot, and D. Ould Abdeslam, "Time-frequency features for sEMG signals classification," in *Proceedings of the 13th International Joint Conference On Biomedical Engineering Systems And Technologies*, vol. 4, pp. 244–249, Valletta, Malta, 2020.

[17] B. Fatimah, P. Singh, A. Singhal, and R. B. Pachori, "Hand movement recognition from sEMG signals using Fourier decomposition method," *Biocybernetics And Biomedical Engineering*, vol. 41, no. 2, pp. 690–703, 2021.

[18] C. Li, D. Cao, and Y. Yua, "Research on improved wavelet denoising method for sEMG signal," in *Proceedings of the 2019 Chinese Automation Congress (CAC2019)*, pp. 5221–5225, Hangzhou, China, November 2019.

[19] S. Kim, J. Kim, M. Kim, S. Kim, and J. Park, "Grasping force estimation by sEMG signals and arm posture: tensor decomposition approach," *Journal Of Bionic Engineering*, vol. 16, no. 3, pp. 455–467, 2019.

[20] S. Liang, Y. Wu, J. Chen et al., "Identification of gesture based on combination of raw sEMG and sEMG envelope using supervised learning and univariate feature selection," *Journal Of Bionic Engineering*, vol. 16, no. 4, pp. 647–662, 2019.

[21] M.-W. Lin, S.-J. Ruan, and Y.-W. Tu, "A 3DCNN-LSTM hybrid framework for sEMG-based noises recognition in exercise," *IEEE Access*, vol. 8, pp. 162982–162988, 2020.

[22] T. Kawase, T. Sakurada, Y. Koike, and K. Kansaku, "A hybrid BMI-based exoskeleton for paresis: EMG control for assisting arm movements," *Journal of Neural Engineering*, vol. 14, no. 1, p. 016015, 2017.

[23] G. G. Peña, L. J. Consoni, W. M. dos Santos, and A. A. G. Siqueira, "Feasibility of an optimal EMG-driven adaptive impedance control applied to an active knee orthosis," *Robotics and Autonomous Systems*, vol. 112, pp. 98–108, 2019.

[24] L. Pan, D. L. Crouch, and H. Huang, "Myoelectric control based on a generic musculoskeletal model: toward a multi-user neural-machine interface," *IEEE Transactions on Neural Systems and Rehabilitation Engineering*, vol. 26, no. 7, pp. 1435–1442, 2018.

[25] T. Kapelner, M. Sartori, F. Negro, and D. Farina, "Neuromusculoskeletal mapping for man-machine interfacing," *Scientific Reports*, vol. 10, no. 1, 2020.

[26] E. C. Yen, "Reconsidering the application scope of fuzzy neural networks," *International Journal of Uncertainty, Fuzziness and Knowledge-Based Systems*, vol. 19, no. 6, pp. 1047–1058, 2011.

[27] S. Wu, M. J. Er, and Y. Gao, "A fast approach for automatic generation of fuzzy rules by generalized dynamic fuzzy neural networks," *IEEE Transactions on Fuzzy Systems*, vol. 9, no. 4, pp. 578–594, 2001.

[28] I. Yun, J. Jeung, H. Lim et al., "Stable bioelectric signal acquisition using an enlarged surface-area flexible skin electrode," *ACS Applied Electronic Materials*, vol. 3, no. 4, pp. 1842–1851, 2021.

[29] E. M. Moaaz, A. M. Mahmoud, A. S. Fayed, M. R. Rezk, and E. M. Abdel-Moety, "Determination of tedizolid phosphate using graphene nanocomposite based solid contact ion selective electrode; green profile assessment by eco-scale and GAPI approach," *Electroanalysis*, vol. 33, no. 8, pp. 1895–1901, 2021.

[30] L. Ma, S. Cheng, and Y. Shi, "Enhancing learning efficiency of brain storm optimization via orthogonal learning design," *IEEE Transactions on Systems, Man, and Cybernetics: Systems*, vol. 51, no. 11, pp. 6723–6742, 2021.

[31] W. Zhang, W. Huang, R. Bai, and D. H. Rui, "Fault diagnosis of wind power gearbox based on IPSO-FNN," in *Proceedings of the 2020 Chinese Automation Congress (CAC 2020)*, pp. 1814–1818, November 2020, Shanghai, China.

[32] H. Yin, S. Lai, G. Xu et al., "Sensitivity analysis of cost elements in rail transit system using EO-FNN," in *Proceedings of the ICBDC 2019: Proceedings Of 2019 4th International Conference On Big Data And Computing*, pp. 287–292, Guangzhou, China, May 2019.

[33] Y. Gao, J. Liu, Z. Wang, and L. Wu, "Interval type-2 FNN-based quantized tracking control for hypersonic flight vehicles with prescribed performance," *Ieee Transactions On Systems Man Cybernetics-Systems*, vol. 51, no. 3, pp. 1981–1993, 2021.